Article

Not peer-reviewed version

Optimized Polymer-Lipid Hybrid Nanoparticles for Enhanced Delivery and Antibacterial Activity of Gentamicin Against Resistant Pathogens

Alaa Eldeen Bakry Yassin * , Faisal Alsuwayyid , Lama Alkhathran , Sabiha Alrouisan , GHadah Alotaibi , Majd Alyaqub , Weam Alsalman , Raghad Alzahrani , Ibrahim Farh , Majed A. Halwani , Shmeylan Al Harbi

Posted Date: 17 January 2025

doi: 10.20944/preprints202501.1317.v1

Keywords: Polymer-Lipid Hybrid Nanoparticles; Gentamicin; double-emulsification/solvent-evaporation technique; Entrapment Efficiency

Article

Optimized Polymer-Lipid Hybrid Nanoparticles for Enhanced Delivery and Antibacterial Activity of Gentamicin Against Resistant Pathogens

Alaa Eldeen Yassin [1,2,*], Faisal Alsuwayyid [1,3], Lama Alkhathran [1], Sabiha Alrouisan [1], Ghadah Alotaibi [1], Majd Alyaqub [1], Weam Alsalman [1], Raghad Alzahrani [2], Ibrahim Farh [1,2], Majed Halawani [1,2] and Shmeylan Al Harbi [1,2,4]

[1] Department of Pharmaceutical Sciences, College of Pharmacy, King Saud bin Abdulaziz University for Health Sciences, Riyadh 11481, Saudi Arabia

[2] King Abdullah International Medical Research Center, Riyadh 11481, Saudi Arabia

[3] Department of Industrial and Molecular Pharmaceutics, Purdue University, 575 Stadium Mall Drive, West Lafayette, IN 47907, USA

[4] Pharmaceutical Care Department, King Abdulaziz Medical City, National Guard Health Affairs, Riyadh 11426, Saudi Arabia

* Correspondence: yassina@ksau-hs.edu.sa

Abstract: Antibiotic resistance is a critical global health concern, driven by biofilm formation and the declining effectiveness of conventional therapies. This study investigates polymer-lipid hybrid nanoparticles (PLNs) as an innovative drug delivery system to enhance the antibacterial efficacy of gentamicin (Gen) while addressing challenges related to its hydrophilicity and encapsulation. Using an optimized double-emulsification/solvent-evaporation technique, PLNs were designed to improve drug entrapment efficiency (EE%) and loading capacity (DL%). The resulting formulations were characterized for particle size, polydispersity, zeta potential, and encapsulation efficiency. Transmitted electron microscopy (TEM) provided insights into particle morphology, while antibacterial activity was tested against multiple bacterial strains, including resistant isolates. The optimized formulation (F4) demonstrated significant improvements, achieving an EE% of 42%, a DL% of 7.2%, and uniform particle sizes (~143.4 nm) with high stability (zeta potential ~-38 mV) and a monodisperse distribution. TEM analysis confirmed Gen encapsulation within the lipid-polymer matrix. F4 exhibited notably enhanced antibacterial performance, particularly against Methicillin-resistant Staphylococcus aureus (MRSA-59) and Pseudomonas aeruginosa (PA-78), with up to a 160-fold reduction in minimum inhibitory/bactericidal concentrations (MIC/MBC) compared to free Gen. These findings underscore the potential of PLNs as a robust platform for targeted drug delivery, offering a promising strategy to combat antimicrobial resistance.

Keywords: polymer-lipid hybrid nanoparticles; gentamicin; double-emulsification/solvent-evaporation technique; entrapment efficiency

1. Introduction

Antibiotic resistance is a major global concern worldwide [1,2]. Over 500,000 infections were caused by antibiotic-resistant bacteria, resulting in more than 30,000 deaths in 2015 in Europe alone as The European Centre for Disease Prevention and Control reported [3]. According to the US Centers for Disease Control and Prevention (CDC), at least 23,000 people in the US die from antibiotic-resistant diseases each year, which impact over two million people annually [4]. As the effect of antibiotics are diminished, infections such as tuberculosis, pneumonia, and gonorrhea are becoming challenging and even impossible to treat [1,5–7].

 doi:10.20944/preprints202501.1317.v1

One of the strategies used by bacteria resistant to antibiotics is the production of biofilms [3,9]. The term “biofilm” first mentioned in a publication authored by Costerton et al. [10]. Later, they defined it as an ordered population of microorganisms that are clinging to a surface and are enclosed in a framework of polymers that the bacteria produces [11]. Chronic infections caused by biofilm-forming bacteria are characterized by persistent tissue damage and inflammation that persists even after multiple antibiotic treatments [12]. Furthermore, mutations, horizontal gene transmission, and anaerobic conditions inside biofilms all contribute to the reduction of antibiotic susceptibility in biofilms [12,13].

Aminoglycosides are broad-spectrum antibiotics with bactericidal activity that were among the first to be identified and used in clinical practice (14). They are mostly used to treat infections brought on by aerobic gram-negative organisms such Serratia spp., Klebsiella pneumoniae, and E. coli [14,15]. They function by blocking the bacterial ribosome's 30S subunit from attaching to messenger RNA, which inhibits the synthesis of proteins [16]. They are frequently used as first-line therapy for diseases like meningitis, endocarditis, and some respiratory infections [15]. However, their clinical use has been limited due to their established toxicities that includes nephrotoxicity, irreversible ototoxicity, and neuromuscular blockade [17–19].

Due to their extremely small size, high surface area-to-volume ratio, and capacity to permeate biological fluids and membranes, nanoparticles (NPs) possess special qualities as drug delivery systems [20,21]. They often increase the duration of drug circulation in the body, increase bioavailability, reduce toxicity, and circumvent the difficulties encountered by traditional administration methods since they are larger than the cut-off size of nephrons [21,22].

Solid lipid nanoparticles (SLNs) are nanoparticulate system made entirely from lipids with melting points higher than common environmental and biological temperatures [23]. Among their many benefits are biocompatibility, protection from harsh environmental conditions, and ease of large-scale synthesis using high-pressure homogenization [24,25]. However, SLNs have drawbacks, including a non-uniform biphasic drug release profile with a high burst effect due to their perfect crystalline structure, which can cause drug expulsion during storage and poor drug loading efficiency limited by the drug's solubility in the particles' lipid matrix [26]. Many attempts in the literature showed the success of drug-loaded SLN in enhancing the activity of many anticancer and antibacterial drugs [27–29].

Polymeric nanoparticles are nanoscale drug carriers that are typically made of biodegradable and biocompatible polymers. They provide more control over drug release, decreased side effects, and improved therapeutic efficacy [30]. Their chemical and physical stability surpasses that of lipid-based nanoparticles, and they offer enhanced stability for drugs, protecting them from degradation by enzymes or environmental factors [31]. Furthermore, their biodegradability nature ensures their safe fate within the body causing no long-term accumulation or toxicity. Polymeric lipid hybrid nanoparticles (PLNs) have been developed to provide advantages over the drawbacks of both lipid and polymeric nanoparticles. The polymer provides better control on drug release while lipids would enhance drug penetration within biological membranes [32,33]. This can result in having nanoparticles with superior biopharmaceutical properties that can be used to achieve the delivery needs of various drugs and drug combinations [34].

Formulating Gen into nanoparticles, which often rely on lipophilic or amphiphilic interactions for drug loading, is extremely difficult due to its great hydrophilicity and low log P (partition coefficient). Effective drug loading is hampered by the mismatch between Gen's water-loving nature and the typically lipophilic character of many nanoparticle carriers [35]. PLN have several advantages that makes it standout compared to other nanoparticle types, but one of its main drawbacks is that is that they poorly encapsulate hydrophilic drugs due to drug leakage from the nanoparticles during the emulsification process [36]. The goal of this study is to optimize the incorporation of Gen into PLN aiming to maximize loading capacity and enhance antibacterial activity while minimizing toxicity.

 doi:10.20944/preprints202501.1317.v1

2. Materials and Methods

2.1. Materials

Gentamycin, polycaprolactone (PCL, Mw 42,000 Da), polyvinyl alcohol, stearic acid, Span 80 and Tween 80 were purchased from Sigma-Aldrich Chemical Co. (St. Louis, MO, USA) through local distributer in Saudi Arabia. Dynasan 118 were purchased from Sasol Germany GmbH (Witten, Germany). Mueller Hinton Agar was obtained from HiMedia Laboratories Pvt. Ltd. (Mumbai, India).

2.2. Methods

2.2.1. Preparation of PLN Drug Formulation

The double-emulsification/solvent-evaporation method described earlier by Omer et al. [37] was employed with minor modifications for the co-encapsulation of Gen into an optimized PLN. Briefly, an organic phase was developed by dissolving certain weights of PCL, stearic acid, and Span 80 in 10 mL chloroform. Certain weights of Gen and Tween 80 was dissolved in 2 mL of water as an aqueous phase. PVA solutions were used as secondary emulsification agent. The aqueous phase was emulsified in the organic phase by probe-sonication for 3 min at 60% voltage efficiency under ice bath utilizing Q700; Qsonica LLC, (Newton, CA, USA). The formed primary emulsion was mixed with certain volume of PCL solution and a secondary emulsion was developed using a second probe-sonication cycle for 5 min. The prepared double emulsion was left overnight under continuous stirring till complete removal of chloroform. The formed PLN was collected by centrifugation for 30 min using 15,000 relative centrifugal force (RCF), and the residue was washed twice to remove un-encapsulated drug. The washed residue was dispersed in a small volume of distilled water and freeze-dried using a Christ freeze-dryer model Beta 2-8 LD Plus (Martin Christ, Germany). The exact composition and formulation parameters are listed in Table 1. In order to increase the Gen entrapment efficiency (EE) %, number of approaches was employed including reducing the volume of water in the double emulsion, increasing the Gen concentration in the aqueous phase, and minimizing the chloroform evaporation time to only one hour by using the rotary evaporator (BUCHI, Flawil, Switzerland). Figure 1 represents a detailed diagram for the finally optimized method.

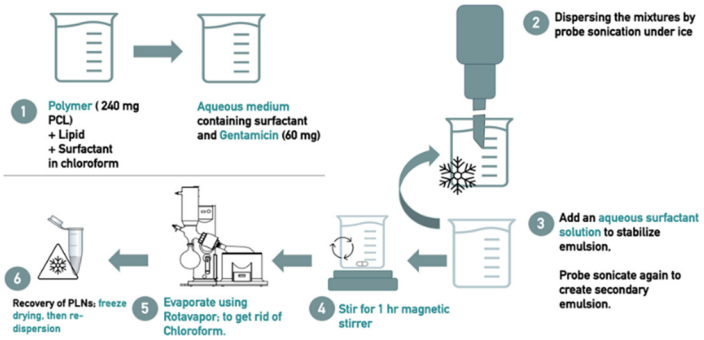

Figure 1. The double-emulsification/solvent-evaporation method diagram.

Table 1. The exact composition of each of the prepared formulations.

Formula Code	Drug	Polymer	Lipids		Primary Surfactant and co-surfactant		Secondary Surfactant	
	Gen	PCL	Dyansan	SA	Tween 80	Span 80	PVA	Tween 80

 doi:10.20944/preprints202501.1317.v1

F0 (Void) *	0	240 mg	25 mg	25 mg	50 mg	50 mg	15 mL (1%)	X
F1	5 mg	150 mg	25 mg	25 mg	25 mg	50 mg	X	30 mL (1%)
F2	5 mg	150 mg	25 mg	25 mg	25 mg	50 mg	40mL (1.5%)	X
F3	40 mg	150 mg	25 mg	25 mg	25 mg	50 mg	40 mL (1%)	X
F4	60 mg	240 mg	25 mg	25 mg	50 mg	50 mg	15 ml (1%)	X

* F0 or Void batch was prepared in accordance with F4 method. *Abbreviations:* Gen, Gentamicin; PCL, Polycaprolactone; SA, Stearic Acid; PVA, Polyvinyl alcohol.

2.2.2. Evaluation of the Physical Characteristics of the Prepared PLN

- Determination of particle size and Polydispersity index:

The particle size and polydispersity of all the formed PLN were measured after dilution with distilled water to almost 0.1% w/v concentration of nanoparticles dispersion utilizing a Brookhaven ZetaPALS (Brookhaven Instruments Corporation, Holtsville, NY, USA). A 90° angle was adjusted for all measurements.

- Determination of zeta-potential:

ZetaPALS was also employed for zeta potential measurement for all the diluted samples applying the mode of the laser Doppler velocimetry.

- Particle morphological features:

A sample from the freeze-dried PLN was weighed and dispersed in distilled water to give 1 mg/L dispersion. The dispersions were sonicated for 10 min. in ultra bath sonicator to render their original particle sizes. Then, one droplet of each dispersion was placed onto a carbon-coated copper grid of 400-mesh and allowed to dry at room temperature. Particle morphology and composition were inspected using a JEM-1400 transmitted electron microscopy [TEM], (JEOL, Tokyo, Japan) at acceleration voltage of 120 KV.

- Drug loading (DL%) and entrapment efficiency (EE)%

Both EE% and DL% were calculated indirectly based on the amount of unentrapped Gen determined in the supernatant of the centrifuged nano-dispersion. Gen was determined by a simple spectrophotometric method. Simply, a set of Gen standard solutions in distilled water was prepared by in concentration range from 25 to 100 µg/mL. A standard calibration curve was constructed after measuring the UV absorbance at λmax = 255 nm utilizing a Thermo Fisher Scientific Evolution 60S UV/Visible Spectrophotometer (Waltham, Massachusetts, United States). The standard curve showed high linearity in this concentration range with R^2 value = 0.9983. The method was validated by repeating the standard curve at 3 different times within the same day (intra-day) and at three different days (inter-day). The EE% and DL% for each formulation were calculated using the following equations:

$$\mathbf{EE\%} = \frac{\boldsymbol{initial\ drug\ weight - unentrapped\ free\ drug}}{\boldsymbol{initial\ drug\ weight}} \boldsymbol{X}\ \mathbf{100} \quad (1)$$

$$\mathbf{DL\%} = \frac{\boldsymbol{initial\ drug\ weight - unentrapped\ free\ drug}}{\boldsymbol{initial\ drug\ weight + weight\ of\ PCL + weight\ of\ lipids}} \boldsymbol{X}\ \mathbf{100} \quad (2)$$

- Physical stability of the prepared PLN:

PLN dispersion 1% in distilled water from F4 was stored in refrigerator for 25 days. Samples were taken periodically and the particle size and PDI were determined for each sample.

 doi:10.20944/preprints202501.1317.v1

2.2.3. Evaluation of the Antibacterial Activity

- Tested bacteria and growth conditions:

We evaluated a range of bacterial strains, including both ATCC and clinical isolates, representing gram-positive and gram-negative species. The bacteria were initially cultured from glycerol stocks stored at -40°C and plated on Luria-Bertani (LB) agar, followed by incubation at 37°C for 18-20 hours to obtain fresh cultures. For the microtiter minimum inhibitory concentration (MIC) assay, Mueller-Hinton Broth (MHB) was used to propagate the bacteria. Subsequently, the minimum bactericidal concentration (MBC) was determined by performing the assay on Mueller-Hinton Agar (MHA) plates. All experimental plates were incubated at 37°C for 18-20 hours [38].

- Antibacterial assays

1. Minimum inhibitory concentration (MIC)

MIC was determined using a 96-well microtiter plate, following the 2003 EUCAST/ESCMID guidelines with minor modifications [39]. Briefly, 100 µL of MHB was added to each well of the microplate. Two-fold serial dilutions of the Gen Formula were prepared by transferring 100 µL of the formula into the subsequent wells. The concentration range for the Gen Formula was 12.5 to 0.39 µg/mL, while the free Gen was tested at concentrations ranging from 32 to 1 µg/mL. The bacterial inoculum was adjusted to a 0.5 McFarland standard using 0.9% saline and further diluted in MHB to achieve the target bacterial concentration of 5×10^5 CFU/mL in the test wells. MHB alone served as the negative control (sterility check), while the positive control consisted of MHB and the bacterial suspension. The microplates were incubated in a rotary shaker incubator at 90 rpm.

2. Minimum bactericidal concentration (MBC)

Following 18-20 hours of incubation, a loopful from each test well was transferred onto Mueller-Hinton Agar (MHA) plates using a 1µL inoculating loop. The plates were then incubated for an additional 18-20 hours. The concentration at which 99% inhibition was observed was recorded as the MBC.

3. Results

3.1. Formulations and Method Development

Table 1 shows the exact modifications and difference between the four formulations. Four PLN formulations were prepared varying a number of factors including; drug to PCL ratio, lipids to PCL ratio, the secondary surfactant type and volume, and the amount of Tween 80. The variation in those factors was attempted to improve the EE% of Gen and the characteristics of the produced NPs. The double emulsification–solvent evaporation method was employed in the preparation of PLN. In formulation 4, rota-evaporator was used to shorten the time of chloroform removal as well as the volume of the aqueous phase was tremendously reduced in order to minimize the escape of Gen into the aqueous phase and subsequently increase the EE%. Figure 1 represents a diagram illustrating the method employed for PLN preparation.

3.2. Polymer-Lipid Hybrid Nanoparticle Characterization

3.2.1. Particle Size and Polydispersity Index

All formulations displayed nanoparticle sizes ranging from 143.4 to 339.9 nm, with polydispersity (PDI) indices between 0.18 and 0.9 as shown in Table 2 and Figure 2. The particle size was influenced by the type and concentration of the secondary surfactant. Both F3 and F4, which were formulated with 1% PVA as the secondary surfactant, showed particle sizes of 251.5 nm and 143.4 nm, respectively. These sizes were notably smaller compared to F1 and F2. When the concentration of Tween 80 was doubled to equalize Span 80 and the volume of PVA was reduced from 40 mL (as in F3) to 15 mL (as in F4), a significant decrease in particle size was observed. In

 doi:10.20944/preprints202501.1317.v1

contrast, using 1% Tween 80 as the secondary surfactant (in F1) led to a higher PDI of 0.9. However, all formulations containing PVA demonstrated excellent particle size uniformity, as indicated by PDI values ≤ 0.25. This is also clear from the size distribution curves represented in Figure 2 C&D where they display single narrow peaks indicating high uniformity in particle sizes.

Table 2. The measurements for each formulation characteristics: mean particle size, polydispersity index (PDI), zeta potential, percent entrapment efficiency (EE%), and drug loading (DL%).

Formulation	Drug:Polymer ratio	Mean particle size (nm) (Mean ± SD)	PDI	Zeta Potential (mV)	EE %	DL%
F0 (Void)	-	178.1 (± 4.50)	0.34	-	-	-
F1	1:30	317.43(±11.85)	0.9	- 38.0	1.7%	0.04%
F2	1:30	339.98 (± 3.81)	0.18	- 38.1	2.4%	0.06%
F3	1:3.75	251.56 (± 3.14)	0.21	-11.9	4.8%	0.8%
F4	1:4	143.42 (± 3.69)	0.25	- 37.9	42.1%	7.2%

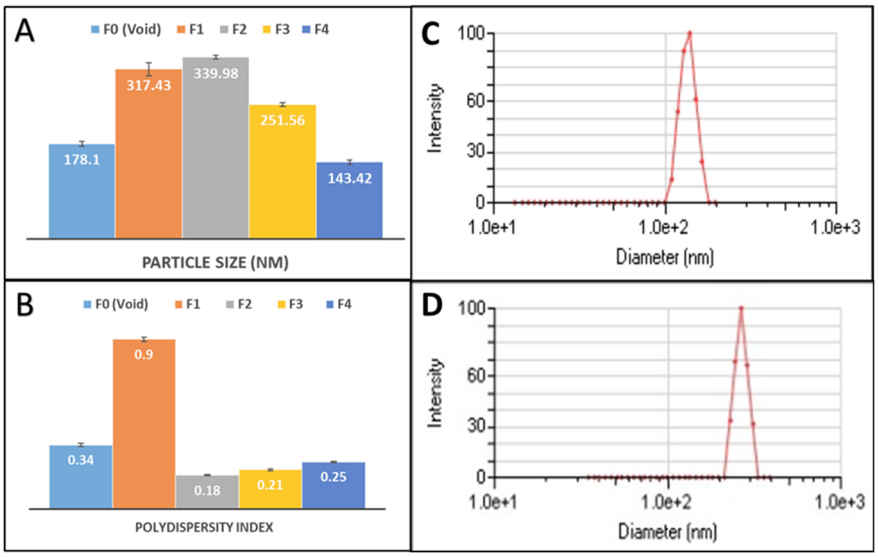

Figure 2. The mean of particle size and polydispersity index (PDI) for all PLN formulations. Notes: (A) The mean ± standard deviation in nm of the particle size for all formulations, (B) The mean ± standard deviation of the polydispersity index (PDI) for all formulations, (C) DLS spectrum showing light scattering intensity percentages of F4, (D) DLS spectrum showing light scattering intensity percentages of F3.

3.2.2. Zeta Potential

Figure 3 illustrates the zeta potential values for the four formulations. All formulations displayed similar values around -38 mV, except for F3, which had a zeta potential of -11.94 mV. The high zeta potential in the other formulations indicates strong particle stability and resistance to aggregation. In contrast, the lower value for F3 suggests it may be more susceptible to aggregation, potentially resulting in a shorter shelf life and diminished performance.

 doi:10.20944/preprints202501.1317.v1

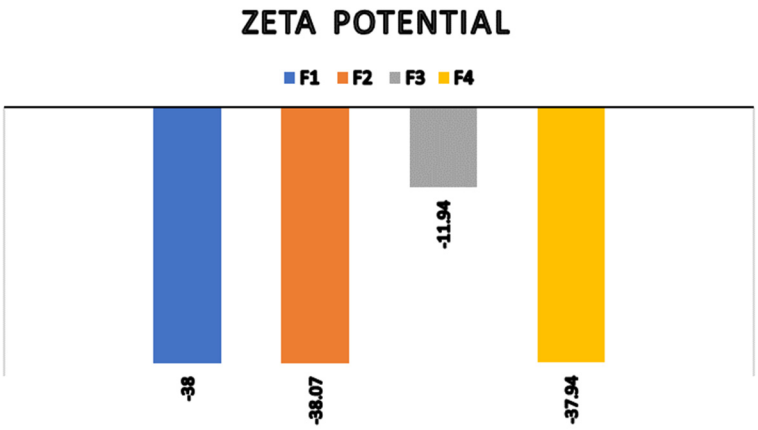

Figure 3. Histogram of the zeta potential values for all PLN formulations.

3.2.3. Drug Loading (DL%) and Entrapment Efficiency (EE%)

The encapsulation efficiency (EE%) in F1 was found to be very low, at only 1.7%, presenting a significant challenge. Replacing Tween 80 with 1.5% PVA as the stabilizer in F2 did not result in a noticeable improvement in EE%. Reducing the PVA concentration to 1% and increasing the amount of Gen (40 mg) while lowering the drug-to-PCL ratio in F3 led to a slight increase in EE% to 4.7%, but this was still considered very low. However, by minimizing the water volume in both the primary and secondary emulsions and shortening the time for chloroform removal using a rotary evaporator, a substantial improvement in EE% was observed in F4, reaching 42%. In terms of drug loading (DL%), values were below 1% for all formulations except F4, which had a DL% of 7.2%.

3.2.4. Morphological Analysis

The results presented in Figure 4 provide insightful details regarding the morphology and structure of F4 PLN (lipid-polymer conjugate particles) across different magnification levels. Image A offers a broad overview of the particle distribution, revealing a dense population of particles with relatively uniform sizes. This size range is notably smaller than those observed through light scattering techniques, which likely highlights the superior resolution and sensitivity of the imaging method employed. The particles exhibit spherical to slightly oval shapes, typical for lipid-polymer conjugate particles. Images B, C, and D provide more detailed views of selected particles, showing variations in black and white intensity. The presence of varying black and white intensities within the particles suggests the potential for heterogeneous internal distribution of components. These intensity differences highlight multiple dark spots in the particles' cores, suggesting the encapsulation of Gen within the particle matrices.

 doi:10.20944/preprints202501.1317.v1

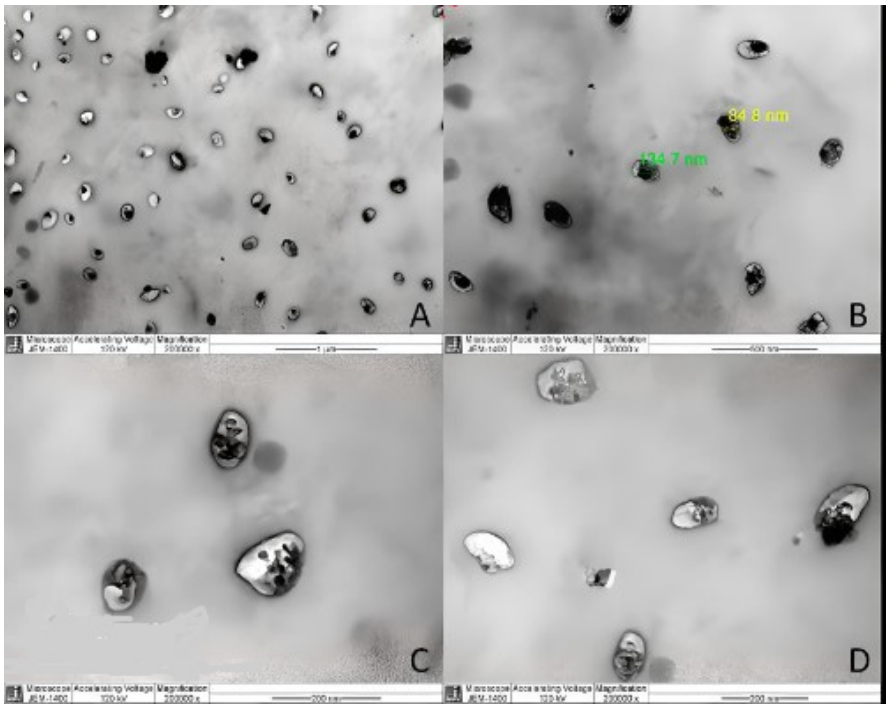

Figure 4. TEM Micrographs of the Gentamicin-Loaded PLN Formulation (F4). Notes: (A) Wide-field view showing a high density of particles. (B) Closer view with particle diameter measurements. (C, D) Higher magnification focusing on individual particles.

3.3. Physical Stability of PLN

Figure 5 illustrates the change in both particle sizes and PDIs with time upon storage of 1% dispersion of F4 in distilled water in a refrigerator for 25 days. As shown in Figure 5 A, the particle size increased to 363 nm after 6 days and then reduced to 308 nm at the end of the 25 days. However the PDI gradually reduced reaching 0.09 at the end of the 25 days indicating excellent particle uniformity or a monodisperse (Figure 5 B).

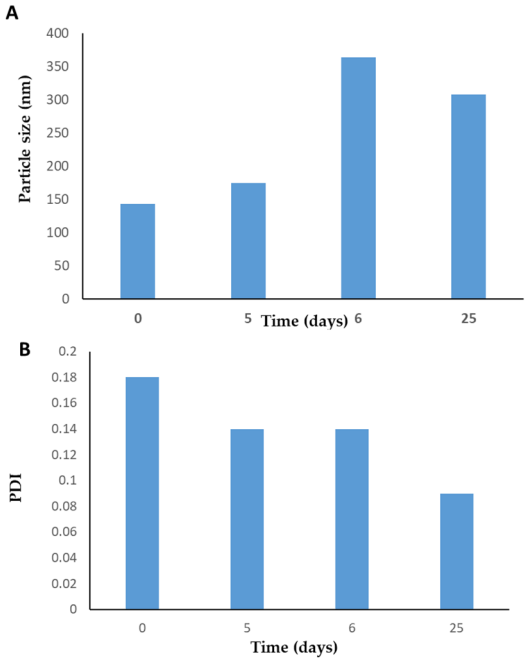

Figure 5. Physical stability of PLN F4 aqueous dispersion for 25 days. A represents change in particle sizes, B represents the change in PDI.

 doi:10.20944/preprints202501.1317.v1

3.4. Antimicrobial Analysis

The antibacterial activity of the optimized PLN formulation, F4, was evaluated by comparing its MIC and MBC values to those of pure Gen at equivalent concentrations against seven bacterial strains, including two ATCC strains and five clinical isolates, two of which were resistant to Gen. The results, summarized in Table 3, highlight the enhanced efficacy of the F4 formulation. Notably, F4 reduced the MIC of Methicillin-resistant S. aureus (MRSA-59), a resistant clinical isolate, by more than 80-fold (3.125 mg/L) compared to free Gen (256 mg/mL), while the MBC was reduced by over 160-fold. Against the clinical isolate Pseudomonas aeruginosa (PA-78), F4 significantly lowered both MIC and MBC values by more than four-fold. Similarly, for the resistant clinical isolate E. coli (EC-219), F4 achieved a more than two-fold reduction in both MIC and MBC values. However, for E. coli ATCC-25922, MRSA-60, and EC-157 strains, no significant reduction in MIC or MBC was observed with the F4 formulation compared to free Gen. These results underscore the potential of F4 in enhancing antibacterial activity, particularly against resistant strains.

Table 3. Antibacterial Activity of gentamicin-loaded polymer-lipid hybrid nanoparticles formulation (F4).

No.	Bacteria	AST Profile	Free GEN (mg/L)		F4 Formula (mg/L)	
			MIC	MBC	MIC	MBC
1	***Staphylococcus aureus* ATCC 29213**	**Susceptible**	2	4	0.78	1.56
2	**Methicillin-resistant *S. aureus* MRSA-59**	Resistant	256	512	3.125	3.125
3	**MRSA-60**	Susceptible	2	4	1.56	3.125
4	***Escherichia coli* ATCC 25922**	Susceptible	2	4	1.56	3.125
5	***E. coli* EC-157**	Susceptible	2	4	1.56	3.125
6	***E. coli* EC-219**	Resistant	8	16	3.125	6.25
7	***Pseudomonas aeruginosa* PA-78**	Susceptible	8	16	1.56	3.125

Gen: gentamicin; MIC: minimum inhibitory concentration; MBC: minimum bactericidal concentration. AST profile: Antibiotic susceptibility Test, which are recorded according to The European Committee on Antimicrobial Susceptibility Testing. Breakpoint tables for interpretation of MICs and zone diameters. Version 13.0, 2023. http://www.eucast.org, Access Date: 20 November 2023.

4. Discussion

The observed nanoparticle sizes and PDIs align with the trend reported in the literature, where surfactant selection and concentration play crucial roles in determining the final characteristics of nanoparticles. In particular, particle size and distribution can be significantly influenced by the choice of surfactants used during the formulation process, as well as their concentration [40]. One of the key findings in this study is the impact of the secondary surfactant on particle size. Specifically, formulations containing PVA as a secondary surfactant, such as F2, F3 and F4, displayed smaller PDIs and particle sizes. Reducing the concentration of PVA to 1%, as in F3 and F4, resulted in significant reduction in particle sizes compared with F2 prepared using 1.5% PVA. This result is consistent with findings from several studies that suggest higher concentrations of PVA can increase the viscosity of the formulation, thereby hindering the dispersion of nanoparticles and leading to larger sizes [41,42]. On the other hand, the formulation using 1% Tween 80 as a secondary surfactant (F1) exhibited the largest particle size and the highest PDI. This is in line with literature that suggests that Tween 80, while effective at stabilizing nanoparticles, can result in a broader size distribution at higher

 doi:10.20944/preprints202501.1317.v1

concentrations [43,44]. The higher PDI observed in F1 indicates greater heterogeneity in the nanoparticle size distribution, which is typically a result of insufficient stabilization or aggregation during formulation. The results regarding particle size uniformity are promising, as all formulations containing PVA (i.e., F3 and F4) displayed excellent particle size uniformity, as indicated by PDI values ≤ 0.25. This finding aligns with the literature, where PVA is frequently employed as a stabilizer due to its excellent ability to reduce particle aggregation and enhance dispersion, resulting in narrower size distributions [45,46].

Particle size emerges as a pivotal factor influencing both the nanoparticles' systemic circulation longevity and their capacity for passive accumulation within tissues (47). Previous studies have highlighted the substantial advantages of nanoparticles falling within the size range of approximately 150 nm for effective systemic drug delivery [47,48]. Our optimum formulation, F4, showed particle size close to this range indicating its superior quality and suitability for Gen delivery.

The zeta potential values presented in Figure 3 provide important insights into the physical stability and aggregation resistance of the four formulations. Zeta potential is a critical parameter for understanding the stability of colloidal systems, as it reflects the electrostatic repulsion between particles in suspension. In this case, all the formulations exhibited zeta potential values close to -38 mV, indicating that they possess a high degree of stability. This high negative charge suggests a significant electrostatic repulsion between particles, which would prevent aggregation and enhance the long-term stability of the formulations. Similar findings have been reported by other studies, where zeta potential values in the range of -30 to -40 mV were associated with increased stability of colloidal dispersions [49,50].

This low DL% and EE% are often attributed to the limited solubility of the drug in the carrier, inefficient encapsulation processes, or the rapid diffusion of the drug into the aqueous phase during formulation. Studies have highlighted that achieving a high DL% requires careful optimization of the drug-to-polymer ratio, solvent evaporation time, and stabilizer concentration [5–53]. In this case, the use of lower PVA concentrations in F1 to F3 likely did not provide sufficient stabilization of the nanoparticles, which may have hindered the encapsulation efficiency and subsequently led to a low drug loading. The significant improvement in DL% and EE% observed in F4, can likely be attributed to the optimization of the formulation conditions. Reducing the water volume in both the primary and secondary emulsions, doubling the amount of the primary emulsion stabilizer, Tween 80, and shortening the chloroform removal time may have reduced drug loss during the process and maintained a higher concentration of the drug within the nanoparticles. This result aligns with findings by Liu et al. [54], who demonstrated that reducing the volume of the aqueous phase during emulsification can limit the drug's diffusion into the surrounding water, thus improving drug loading. Additionally, the time-efficient chloroform evaporation process is known to aid in the preservation of drug encapsulation by preventing excessive leaching of the drug into the external phase [52]. These adjustments were guided by previous studies and preliminary experiments, which demonstrated more efficient formation of PLNs with higher entrapment efficiency [55].

The spherical to slightly oval shapes of the particles observed in TEM images supports the notion that these particles are indeed lipid-polymer conjugates, as similar particles have been previously described in the literature for their structural and functional properties [56,57]. These intensity differences are indicative of regions with higher electron density, which may correspond to encapsulated substances or areas of lipid aggregation [58]. The dark spots observed in the cores of the particles are particularly noteworthy, as they imply the encapsulation of Gen within the lipid-polymer matrices. The matrix structure likely contributes to the stability of the encapsulated Gen, as lipid-polymer conjugates are known to offer both protection and controlled release properties [56]. This characteristic is particularly advantageous in the context of drug delivery systems, where the aim is to ensure that the active compound is delivered efficiently to the target site without being prematurely released.

The increase in particle size of the F4 dispersion in water over a 25-day storage period may be explained by water diffusion into the PCL matrix, leading to swelling [59]. Another plausible reason

 doi:10.20944/preprints202501.1317.v1

is Ostwald ripening, a process commonly observed in lipid-based nanoparticles, particularly when the particles lack sufficient stabilization [60]. Meanwhile, the gradual reduction in PDI to 0.09 by day 25 reflects the transition of the dispersion into a highly monodisperse state. This enhanced uniformity over time could result from the particles settling into a more homogeneous distribution. Research indicates that stabilizers such as surfactants or polymers play a vital role in promoting particle uniformity by preventing aggregation [61].

The enhanced antibacterial efficacy of the optimized polycaprolactone nanoparticle (PLN) formulation, F4, encapsulating gentamicin (Gen), against various bacterial strains, including antibiotic-resistant isolates, demonstrates the significant potential of nanoparticle-based drug delivery systems in combating resistant infections.

F4 achieved a remarkable reduction in MIC and MBC values against Methicillin-resistant Staphylococcus aureus (MRSA-59), with MIC decreasing by over 80-fold and MBC by more than 160-fold compared to free Gen. This improvement can be attributed to the enhanced penetration and sustained release properties of the nanoparticle formulation, which allow higher intracellular antibiotic concentrations and help overcome resistance mechanisms. Similar findings have been reported for Gen combined with threonine amino acid, which significantly enhanced bactericidal activity against MRSA USA300_FPR3757 [62]. Additionally, Gen-loaded chitosan nanoparticles have demonstrated enhanced efficacy against S. aureus, further supporting the observed results [63].

Against Pseudomonas aeruginosa (PA-78), F4 reduced both MIC and MBC values by more than four-fold. The resistance of P. aeruginosa is often attributed to its robust defense mechanisms, such as efflux pumps and biofilm formation. The nanoparticle-based delivery of Gen likely enhances its ability to penetrate biofilms and evade efflux mechanisms, thereby increasing antibacterial activity. This aligns with the findings of Abdelghany et al. [64], who demonstrated that Gen-loaded poly(lactide-co-glycolide) nanoparticles reduced colony-forming units and interleukin-6 levels in a peritoneal murine infection model of P. aeruginosa, despite higher MIC and MBC values. Furthermore, co-encapsulation of Gen and ascorbic acid into chitosan nanoparticles has been reported to significantly reduce MIC and MBC against P. aeruginosa [65]. Enhanced efficacy of Gen has also been demonstrated with Gen-conjugated gold nanoparticles against multiple bacterial strains [66,67].

For the resistant clinical isolate Escherichia coli (EC-219), F4 achieved more than a two-fold reduction in both MIC and MBC values. This improvement can be attributed to better interaction of the nanoparticles with bacterial membranes and the controlled release of Gen, maintaining therapeutic concentrations over time. A recent study reported that co-encapsulation of Gen with thymoquinone into liposomes significantly reduced MIC and MBC values against resistant E. coli strains by four-fold [68]. However, for E. coli ATCC-25922, MRSA-60, and EC-157 strains, no significant reduction in MIC or MBC was observed with the F4 formulation compared to free Gen. This indicates that the efficacy of nanoparticle-encapsulated antibiotics may vary depending on specific bacterial characteristics, such as membrane permeability, the presence of resistance genes, or biofilm-forming capabilities. Similar findings were observed with other Gen-nanoparticles, such as calcium carbonate and poly(lactide-co-glycolide), which showed MIC values comparable to pure Gen [69,70]. These results highlight the need for tailored approaches when developing nanoparticle-based therapies to target different bacterial pathogens effectively.

5. Conclusions

The emulsification-solvent evaporation method was successfully optimized to achieve a high loading of Gen into PLN, addressing the significant challenge posed by the drug's extreme hydrophilicity. Key modifications, such as reducing water volume, increasing surfactant concentration, and shortening the organic solvent removal time, effectively minimized drug loss and enhanced drug retention within the nanoparticles. The resulting nanoparticles exhibited highly uniform, small particle sizes and demonstrated excellent physical stability. This study underscores the critical influence of surfactant type and concentration on nanoparticle formation, as reflected in

 doi:10.20944/preprints202501.1317.v1

the observed particle sizes and PDIs. The use of PVA, particularly at lower concentrations, produced smaller and more uniform nanoparticles, highlighting its effectiveness as a stabilizer. The high zeta potential values across formulations confirm strong physical stability, while TEM analysis verified the successful encapsulation of Gen within the nanoparticle core. The optimized F4 PLN formulation exhibited exceptional antibacterial efficacy, particularly against resistant bacterial strains such as MRSA-59, showcasing its promise as a potent therapeutic option. This study introduced a novel approach for preparing Gen-loaded PLN, characterized by distinct physical properties, high drug loading capacity, and significantly improved antibacterial activity against resistant pathogens. These findings underscore the potential of this formulation strategy in developing tailored nanoparticles, tackling the critical challenge of antimicrobial resistance, and paving the way for effective therapeutic interventions.

Author Contributions: Conceptualization, A.E.Y. and M.H.; methodology, F.A., R.A., I.F., L.A., S.A.; software, G.A., M.A., W.A.; validation, S.H., M.H. and F.A.; formal analysis, I.F., L.A., R.A.; investigation, A.E.Y., M.H.; resources, S.H., A.E.B.; data curation, F.A., R.A., G.A.; writing—original draft preparation, L.A., S.A., M.A., R.A., W.A. ; writing—review and editing, A.E.Y., M.H., S.H.; visualization, G.A., S.A., W.A.; supervision, I.F., F.A., R.A.; project administration, A.E.Y.; funding acquisition, A.E.Y. All authors have read and agreed to the published version of the manuscript.

Funding: This work was funded by King Abdullah International Medical Research Center (KAIMRC), Ministry of National Guard-Health Affairs (Grant Nos. RC20/109/R and SP22R/226/10). The funding agency had no role in the decision to publish or prepare the manuscript.

Institutional Review Board Statement: Not applicable.

Informed Consent Statement: Not applicable.

Data Availability Statement: Data is contained within the article.

Conflicts of Interest: The authors declare no conflicts of interest. The funders had no role in the design of the study; in the collection, analyses, or interpretation of data; in the writing of the manuscript; or in the decision to publish the results.

References

1. Murray, C.J.L. et al.; Antimicrobial Resistance Collaborators. Global burden of bacterial antimicrobial resistance in 2019: a systematic analysis. *The Lancet* **2022**, 399, Issue 10325, 629 – 655.
2. Prestinaci, F.; Pezzotti, P.; Pantosti, A. Antimicrobial resistance: a global multifaceted phenomenon. *Pathog Glob Health* **2015**, 109(7), 309-18. doi: 10.1179/2047773215Y.0000000030.
3. Cassini, A.; Högberg, L.; Plachouras, D.; Quattrocchi, A.; Hoxha, A.; Simonsen, G.S.; et al. Attributable deaths and disability-adjusted life-years caused by infections with antibiotic-resistant bacteria in the EU and the European Economic Area in 2015: a population-level modelling analysis. *Lancet Infect Dis* **2019**, 19(1), 56–66.
4. Centres for Disease Control and Prevention, US Department of Health and Human Services. Antibiotic resistance threats in the United States. Atlanta: CDC; **2013**. Available from: https://www.cdc.gov/antimicrobial-resistance/media/pdfs/ar-threats-2013-508.pdf?CDC_AAref_Val=https://www.cdc.gov/drugresistance/pdf/ar-threats-2013-508.pdf (accessed on 16-1-2025).
5. Antimicrobial Resistance. WHO; **2023**; Available from: https://www.who.int/news-room/fact-sheets/detail/antimicrobial-resistance (Accessed 16-1-2025)
6. Chinemerem Nwobodo, D.; Ugwu, M.C.; Oliseloke Anie, C.; Al-Ouqaili, M.T.S.; Chinedu Ikem, J.; Victor Chigozie, U.; Saki, M. Antibiotic resistance: The challenges and some emerging strategies for tackling a global menace. *J Clin Lab Anal* **2022**, 36(9), e24655. doi: 10.1002/jcla.24655.
7. Nadgir, C.A.; Biswas, D.A. Antibiotic Resistance and Its Impact on Disease Management. *Cureus* **2023,** 15(4), e38251. doi: 10.7759/cureus.38251.

8. Cepa,s V.; López, Y.; Muñoz E, Rolo D, Ardanuy C, Martí S, et al. Relationship between Biofilm Formation and Antimicrobial Resistance in Gram-Negative Bacteria. Microb Drug Resist. 2019 Jan 1;25(1):72–9.
9. 9. Sharma S, Mohler J, Mahajan, S.D.; Schwartz, S.A.; Bruggemann, L.; Aalinkeel, R. Microbial Biofilm: A Review on Formation, Infection, Antibiotic Resistance, Control Measures, and Innovative Treatment. *Microorganisms* **2023**, 11(6), 1614. doi: 10.3390/microorganisms11061614.
10. Costerton, J.W.; Geesey, G.G.; Cheng, K.J. How bacteria stick. *Sci Am* **1978**, 238, 86–95. doi: 10.1038/scientificamerican0178-86.
11. Costerton, J.W.; Stewart, P.S.; Greenberg, E.P. Bacterial biofilms: A common cause of persistent infections. *Science* **1999**, 284, 1318–1322. doi: 10.1126/science.284.5418.1318.
12. Høiby, N.; Ciofu, O.; Johansen, H.K.; Song, Z.J.; Moser, C.; Jensen, P.Ø. et al. The clinical impact of bacterial biofilms. *Int J Oral Sci* **2011**, 3(2), 55–65.
13. Michaelis, C.; Grohmann, E. Horizontal Gene Transfer of Antibiotic Resistance Genes in Biofilms. *Antibiotics (Basel)* **2023**, 12(2), 328. doi: 10.3390/antibiotics12020328.
14. Krause, K.M.; Serio, A.W.; Kane, T.R.; Connolly, L.E. Aminoglycosides: An overview. *Cold Spring Harb Perspect Med* **2016**, 6(6), a027029. doi:10.1101/cshperspect.a027029
15. Germovsek, E; Barker, C.I.; Sharland, M. What do i need to know about aminoglycoside antibiotics? *Arch Dis Child Educ Pract Ed* **2017**, 102(2), 89–93.
16. Bernd, B.; Cooper, M.A. Aminoglycosides antibiotics in the 21st century. *ACS Chemical Biology* **2013**, 8(1), 105-115. doi: 10.1021/cb3005116
17. Xie, J.; Talaska, A.E.; Schacht, J. New developments in aminoglycoside therapy and ototoxicity. *Hear Res* **2011**, 281(1-2), 28-37. doi: 10.1016/j.heares.2011.05.008.
18. Streetman, D.S.; Nafziger, A.N.; Destache, C.J.; Bertino, A.S. Jr. Individualized pharmacokinetic monitoring results in less aminoglycoside-associated nephrotoxicity and fewer associated costs. *Pharmacotherapy* **2001**, 21, 443–451. doi: 10.1592/phco.21.5.443.34490.
19. Fausti, S.A.; Frey, R.H.; Henry, J.A.; Olson, D.J.; Schaffer, H.I. Early detection of ototoxicity using high-frequency, tone burst-evoked auditory brainstem responses. *J Am Acad Audiol* **1992**, 3, 397–404.
20. Sabourian, P.; Yazdani, G.; Ashraf, S.S.; Frounchi, M.; Mashayekhan, S.; Kiani, S. et al. Effect of Physico-Chemical Properties of Nanoparticles on Their Intracellular Uptake. *Int J Mol Sci* **2020**, 21, 8019. doi:10.3390/ijms21218019
21. Gelperina, S.; Kisich, K.; Iseman, M.D.; Heifets, L. The potential advantages of nanoparticle drug delivery systems in chemotherapy of tuberculosis. *Am J Respir Crit Care Med* **2005**, 172(12), 1487-1490. doi: 10.1164/rccm.200504-613PP.
22. Patra, J. K.; Das, G.; Fraceto, L. F.; Campos, E. V. R.; Rodriguez-Torres, M. D. P.; Acosta-Torres, L. S.; Diaz-Torres, L. A.; Grillo, R.; Swamy, M. K.; Sharma, S.; Habtemariam, S.; Shin, H. S. Nano based drug delivery systems: recent developments and future prospects. *J Nanobiotechnol* **2018**, 16, 71. https://doi.org/10.1186/s12951-018-0392-8
23. Yassin, A.E.B.; Albekairy, A.; Alkatheri, A.; Sharma, R.K. Anticancer-loaded solid lipid nanoparticles: high potential advancement in chemotherapy. *Digest J of Nanomat and Biostructures* **2013**, 8(2), 905 – 916.
24. Rajpoot, K. Solid lipid nanoparticles: a promising nanomaterial in drug delivery. *Curr Pharm Des* **2019**, 25 (37), 3943-3959.
25. Ghasemiyeh, P; Mohammadi-Samani, S. Solid lipid nanoparticles and nanostructured lipid carriers as novel drug delivery systems: applications, advantages and disadvantages. *Res Pharm Sci* **2018**, 13(4), 288-303. doi: 10.4103/1735-5362.235156.
26. Müller, R.H.; Mäder, K.; Gohla, S. Solid lipid nanoparticles (SLN) for controlled drug delivery – a review of the state of the art. *Eur J Pharm Biopharm* **2000**, 50(1), 161–177.
27. Aljihani, S.A.; Alehaideb, Z.; Alarfaj, R.E.; Alghoribi, M.F.; Akiel, M.A.; Alenazi, T.H.; Al-Fahad, A.J.; Al Tamimi, S.M.; Albakr, T.M.; Alshehri, A.; Alyahya, S.M.; Yassin, A.E.B.; Halwani, M.A. Enhancing azithromycin antibacterial activity by encapsulation in liposomes/liposomal-N-acetylcysteine formulations against resistant clinical strains of Escherichia coli. *Saudi J Biol Sci* **2020**, 27(11), 3065-3071. doi: 10.1016/j.sjbs.2020.09.012.

28. Serpe, L.; Catalano, M.G.; Cavalli, R.; Ugazio, E.; Bosco, O.; Canaparo, R.; Muntoni, E.; Frairia, R.; Gasco, M.R.; Eandi, M.; Zara, G.P. Cytotoxicity of anticancer drugs incorporated in solid lipid nanoparticles on HT-29 colorectal cancer cell line. *Eur J Pharm Biopharm* **2004**, 58(3), 673-80. doi: 10.1016/j.ejpb.2004.03.026.
29. Battaglia, L.; Serpe, L.; Muntoni, E.; Zara, G.; Trotta, M.; Gallarate, M. Methotrexate-loaded SLNs prepared by coacervation technique: in vitro cytotoxicity and in vivo pharmacokinetics and biodistribution. *Nanomedicine (Lond)* **2011**, 6(9), 1561-1573. doi: 10.2217/nnm.11.52.
30. Lai, P.; Daear, W.; Löbenberg, R.; Prenner, E. J. Overview of the preparation of organic polymeric nanoparticles for drug delivery based on gelatine, chitosan, poly (d, l -lactide-co-glycolic acid) and polyalkylcyanoacrylate. *Colloids and Surfaces B: Biointerfaces* **2014**, 118, 154–163. https://doi.org/10.1016/j.colsurfb.2014.03.017.
31. El-say, K. M.; El-sawy, H. S. Polymeric nanoparticles: Promising platform for drug delivery. *Int J Pharm* **2017**, 528, 675–691. https://doi.org/10.1016/j.ijpharm.2017.06.052.
32. Hallan, S.S.; Kaur, P.; Kaur, V.; Mishra, N.; Vaidya, B. Lipid polymer hybrid as emerging tool in nanocarriers for oral drug delivery. *Artif Cells Nanomed Biotechnol* **2016**, 44(1), 334-49. doi: 10.3109/21691401.2014.951721.
33. Sivadasan, D.; Sultan, M.H.; Madkhali, O.; Almoshari, Y.; Thangavel, N. Polymeric Lipid Hybrid Nanoparticles (PLNs) as Emerging Drug Delivery Platform-A Comprehensive Review of Their Properties, Preparation Methods, and Therapeutic Applications. *Pharmaceutics* **2021**, 13(8), 1291. doi: 10.3390/pharmaceutics13081291.
34. Zhang, L.; Chan, J.M.; Gu, F.X.; Rhee, J.W.; Wang, A.Z.; Radovic-Moreno, A.F. et al. Self-assembled lipid-polymer hybrid nanoparticles: A robust drug delivery platform. *ACS Nano* **2008**, 2(8), 1696–702.
35. Walker, R. J.; Keating, G. M. Aminoglycosides. In Schwartz , L.B., Sutcliffe, A.I. (Eds.), Antibiotics: Discovery and development, Springer International Publishing: New York City, USA, 2017; pp. 45-60.
36. Cheow, W.S.; Hadinoto, K. Lipid-polymer hybrid nanoparticles with rhamnolipid triggered release capabilities as anti-biofilm drug delivery vehicles. *Particuology* **2012**, 1, 327- 333. https://www.sciencedirect.com/science/article/abs/pii/S0927775710004954
37. Omer, M.E.; Halwani, M.; Alenazi, R.M.; Alharbi, O.; Aljihani, S.; Massadeh, S.; Al Ghoribi, M.; Al Aamery, M.; Yassin, A. E. Novel Self-Assembled Polycaprolactone–Lipid Hybrid Nanoparticles Enhance the Antibacterial Activity of Ciprofloxacin. *SLAS TECHNOLOGY: Translating Life Sciences Innovation* **2020**, 25(6), 598-607. doi:10.1177/2472630320943126
38. CLSI. (2017). M100-S27: Performance Standards for Antimicrobial Susceptibility Testing (27th ed.). Clinical and Laboratory Standards Institute.
39. European Committee for Antimicrobial Susceptibility Testing (EUCAST) of the European Society of Clinical Microbiology and Infectious Disease (ESCMID). Determination of minimum inhibitory concentrations (MICs) of antibacterial agents by broth dilution. *Clin Microbiol Infect* **2003**, 9, 1–7.
40. Bolourchian, N.; Shafiee Panah, M. The Effect of Surfactant Type and Concentration on Physicochemical Properties of Carvedilol Solid Dispersions Prepared by Wet Milling Method. *Iran J Pharm Res* **2022**, 21(1), e126913. doi: 10.5812/ijpr-126913.
41. Kitayama, Y.; Takigawa, S.; Harada, A. Effect of Poly(Vinyl Alcohol) Concentration and Chain Length on Polymer Nanogel Formation in Aqueous Dispersion Polymerization. *Molecules* **2023**, 28(8), 3493. https://doi.org/10.3390/molecules28083493
42. Ekinci, M.; Yeğen, G.; Aksu, B.; İlem-Özdemir, D. Preparation and Evaluation of Poly(lactic acid)/Poly(vinyl alcohol) Nanoparticles Using the Quality by Design Approach. *ACS Omega* **2022**, 7 (38), 33793-33807. DOI: 10.1021/acsomega.2c02141
43. Masarudin, M.J.; Cutts, S.M.; Evison, B.J.; Phillips, D.R.; Pigram, P.J. Factors determining the stability, size distribution, and cellular accumulation of small, monodisperse chitosan nanoparticles as candidate vectors for anticancer drug delivery: application to the passive encapsulation of [14C]-doxorubicin. *Nanotechnol Sci Appl* **2015**, 8, 67-80. doi: 10.2147/NSA.S91785.
44. Filipe, V.; Hawe, A.; Jiskoot, W. Critical evaluation of Nanoparticle Tracking Analysis (NTA) by NanoSight for the measurement of nanoparticles and protein aggregates. *Pharm Res* 2010, 27(5), 796-810. doi: 10.1007/s11095-010-0073-2.

45. Chatterjee; S.; Bhattacharya, S.K. Size-Dependent Catalytic Activity of PVA-Stabilized Palladium Nanoparticles in p-Nitrophenol Reduction: Using a Thermoresponsive Nanoreactor. *ACS Omega* **2021**, 6(32), 20746-20757. doi: 10.1021/acsomega.1c00896.
46. Xiao-ting, C.; Wang, T. Preparation and characterization of atrazine-loaded biodegradable PLGA nanospheres. *Journal of Integrative Agriculture* **2019**, 18(5), 1035–1041. doi: 10.1016/S2095-3119(19)62613-4
47. Danaei, M.; Dehghankhold, M.; Ataei, S.; Hasanzadeh Davarani, F.; Javanmard R.; Dokhani, A.; Khorasani, S.; Mozafari, M.R.. Impact of particle size and polydispersity index on the clinical applications of lipidic nanocarrier systems. *Pharmaceutics* **2018**, 10(2), 57. https://doi.org/10.3390/pharmaceutics10020057
48. Chenthamara, D.; Subramaniam, S.; Ramakrishnan, S.G.; Krishnaswamy, S.; Essa, M.M.; Lin, F.H.; Qoronfleh, M.W. Therapeutic efficacy of nanoparticles and routes of administration. *Biomater Res* **2019**, 23, 20. doi: 10.1186/s40824-019-0166-x.
49. Hu, Y.; Yang, Q.; Kou, J.; Sun, C.; Li, H. Aggregation mechanism of colloidal kaolinite in aqueous solutions with electrolyte and surfactants. *PLoS One* **2020**, 15(9):e0238350. doi: 10.1371/journal.pone.0238350.
50. Rami, M.L.; Meireles, M.; Cabane, B.; Guizard, C. Colloidal stability for concentrated zirconia aqueous suspensions, J Am Ceram Soc **2009**, 92, 50–56, https://doi.org/10.1111/j.1551-2916.2008.02681.x.
51. Pulingam, T.; Foroozandeh, P.; Chuah, J-A.; Sudesh, K. Exploring Various Techniques for the Chemical and Biological Synthesis of Polymeric Nanoparticles. *Nanomaterials* **2022**, 12(3), 576. https://doi.org/10.3390/nano12030576
52. Bohrey, S.; Chourasiya, V.; Pandey, A. Polymeric nanoparticles containing diazepam: preparation, optimization, characterization, in-vitro drug release and release kinetic study. *Nano Convergence* **2016**, 3, 3. https://doi.org/10.1186/s40580-016-0061-2
53. Alkholief, M.; Kalam, M.A.; Anwer, M.K.; Alshamsan, A. Effect of Solvents, Stabilizers and the Concentration of Stabilizers on the Physical Properties of Poly(d,l-lactide-co-glycolide) Nanoparticles: Encapsulation, In Vitro Release of Indomethacin and Cytotoxicity against HepG2-Cell. *Pharmaceutics* **2022**, 14(4), 870. doi: 10.3390/pharmaceutics14040870.
54. Liu, B.; Dong, Q.; Wang, M.; Shi, L.; Wu, Y.; Yu, X.; Shi, Y.; Shan, Y.; Jiang, C.; Zhang, X.; Gu, T.; Chen, Y.; Kong, W. Preparation, characterization, and pharmacodynamics of exenatide-loaded poly(DL-lactic-co-glycolic acid) microspheres. *Chem Pharm Bull (Tokyo)* **2010**, 58(11), 1474-9. doi: 10.1248/cpb.58.1474.
55. Radwan, M.A. In vitro evaluation of polyisobutylcyanoacrylate nanoparticles as a controlled drug carrier for theophylline. *Drug Dev Ind Pharm* **1995**, 21(20), 2371–2375.
56. Gajbhiye, K.R.; Salve, R.; Narwade, M.; Sheikh, A.; Kesharwani, P.; Gajbhiye, V. Lipid polymer hybrid nanoparticles: a custom-tailored next-generation approach for cancer therapeutics. *Mol Cancer* **2023**; 22(1), 160. doi: 10.1186/s12943-023-01849-0.
57. Sultan, M.H.; Moni, S.S.; Madkhali, O.A.; Bakkari, M.A.; Alshahrani, S.; Alqahtani, S.S.; Alhakamy, N.A.; Mohan, S.; Ghazwani, M.; Bukhary, H.A.; Almoshari, Y.; Salawi, A.; Alshamrani, M. Characterization of cisplatin-loaded chitosan nanoparticles and rituximab-linked surfaces as target-specific injectable nano-formulations for combating cancer. *Sci Rep* **2022**, 12(1), 468. doi: 10.1038/s41598-021-04427-w.
58. Mehta, M.; Bui, T.A.; Yang, X.; Aksoy, Y.; Goldys, E.M.; Deng, W. Lipid-Based Nanoparticles for Drug/Gene Delivery: An Overview of the Production Techniques and Difficulties Encountered in Their Industrial Development. *ACS Mater Au* **2023**, 3(6), 600-619. doi: 10.1021/acsmaterialsau.3c00032.
59. Kayan, GÖ; Kayan, A. Polycaprolactone Composites/Blends and Their Applications Especially in Water Treatment. *Chem Engineering* **2023**, 7(6), 104. https://doi.org/10.3390/chemengineering7060104.
60. Musielak, E.; Feliczak-Guzik, A.; Nowak, I. Optimization of the Conditions of Solid Lipid Nanoparticles (SLN) Synthesis. *Molecules* **2022**, 27(7), 2202. doi: 10.3390/molecules27072202.
61. Cortés, H.; Hernández-Parra, H.; Bernal-Chávez, S.A.; Prado-Audelo, M.L.D.; Caballero-Florán, I.H.; Borbolla-Jiménez, F.V.; González-Torres, M.'; Magaña, J.J.; Leyva-Gómez, G. Non-Ionic Surfactants for Stabilization of Polymeric Nanoparticles for Biomedical Uses. *Materials (Basel)* **2021**, 14(12), 3197. doi: 10.3390/ma14123197.
62. Guo, J.; Pan, Z.; Fan, L.; Zhong, Y.; Pang, R.; Su, Y. Effect of Three Different Amino Acids Plus Gentamicin Against Methicillin-Resistant Staphylococcus aureus. *Infect Drug Resist* **2023**, 16, 4741-4754. https://doi.org/10.2147/IDR.S411658.

63. Shi, S.; Lu, W.; Gu, X.; Lin Q. Efficacy of Gentamicin-Loaded Chitosan Nanoparticles Against Staphylococcus aureus Internalized in Osteoblasts. Microb Drug Resist **2024**; 30(5), 196-202. doi: 10.1089/mdr.2023.0066.
64. Abdelghany, S.M.; Quinn, D.J.; Ingram, R.J.; Gilmore, B.F.; Donnelly, R.F.; Taggart, C.C.; Scott, C.J. Gentamicin-loaded nanoparticles show improved antimicrobial effects towards Pseudomonas aeruginosa infection. Int J Nanomed **2012**; 7, 4053-4063. doi: 10.2147/IJN.S34341.
65. Abdel-Hakeem, M.A.; Abdel Maksoud, A.I.; Aladhadh, M.A.; Almuryif, K.A.; Elsanhoty, R.M.; Elebeedy, D. Gentamicin-Ascorbic Acid Encapsulated in Chitosan Nanoparticles Improved In Vitro Antimicrobial Activity and Minimized Cytotoxicity. *Antibiotics (Basel)* **2022**; 11(11), 1530. doi: 10.3390/antibiotics11111530.
66. Ahangari, A.; Salouti, M.; Heidari, Z.; Kazemizadeh, A.R.; Safari, A.A. Development of gentamicin-gold nanospheres for antimicrobial drug delivery to Staphylococcal infected foci. *Drug Deliv* **2013**, 20, 34–39.
67. Mohanta, B.; Chakraborty, A.; Selvara, S.; Roy, A. Bactericidal effect of gentamicin conjugated gold nanoparticles. *Micro Nano Lett* **2020**, 15, 657–661.
68. Alzahrani, R.R.; Alkhulaifi, M.M.; Al Jeraisy, M.; Albekairy, A.M.; Ali, R.; Alrfaei, B.M.; Ehaideb, S.N.; Al-Asmari, A.I.; Qahtani, S.A.; Halwani A, Yassin, A.E.B.; Halwani, M.A.. Enhancing Gentamicin Antibacterial Activity by Co-Encapsulation with Thymoquinone in Liposomal Formulation. *Pharmaceutics* **2024**, 16(10), 1330. https://doi.org/10.3390/pharmaceutics16101330.
69. Maleki Dizaj, S.; Lotfipour, F.; Barzegar-Jalali, M.; Zarrintan, M.H.; Adibkia, K. Physicochemical characterization and antimicrobial evaluation of gentamicin-loaded $CaCO_3$ nanoparticles prepared via microemulsion method. *J Drug Deliv Sci Technol* **2016**, 35, 16–23. https://doi.org/10.1016/j.jddst.2016.05.004
70. Posadowska, U.; Brzychczy-Włoch, M.; Pamuła, E. Gentamicin loaded PLGA nanoparticles as local drug delivery system for the osteomyelitis treatment. *Acta Bioeng Biomech* **2015**, 17, 41–48. https://doi.org/10.5277/ABB-00188-2014-02